Quantitative visualization of weak shock waves by phase-shift holographic interferometry

Toshiharu Mizukaki[1], Harald Kleine[2], and Kazuyoshi Takayama[1]

[1] Shock Wave Research Center, Institute of Fluid Science, Tohoku University, Sendai, Japan
[2] Department of Aeronautics and Space Engineering, Faculty of Engineering, Tohoku University, Sendai, Japan

Abstract. By applying two-reference beam interferometry together with digital data processing, a correspondingly modified double exposure holographic interferometer has been used to measure the density distribution in flow fields generated by very weak shock waves. The weak shock waves were generated by the explosion of milligram charges of silver azide, which were ignited by a pulsed Nd:YAG laser. With the help of this technique, density variations in a flow field associated with a shock Mach number $M_s = 1.0007$ were visualized and quantified. Phenomena that generated a sound intensity of 135dB could be resolved.

1 Introduction

Holographic interferometry is a widely used technique for the visualization of compressible fluid flow [1] [2]. This technique is a special form of so-called reference beam interferometry, which is a class of methods that allows one to visualize the density distribution in a compressible flow [2]. If density changes occur within the test object the phase ϕ of a traversing light beam is modified. The resulting phase differences $\Delta\phi$ are indicated on a recording screen by the appearance of new interference fringes (infinite fringe mode) or by the distortion of already existing ones (finite fringe setting). The relationship between the phase difference $\Delta\phi$ and the refractive index $n(x, y, z)$ of the fluid is [2]

$$\Delta\phi(x, y) = \frac{2\pi}{\lambda} \int_{z_1}^{z_2} [n(x, y, z) - n_0] dz, \tag{1}$$

where λ is the wavelength of the light source and n_0 is a known reference refractive index. z is the coordinate in the direction of light beam propagation.

This relationship is considerably simplified when the object is homogeneous along the line of observation, i.e., $n \neq n(z)$. In this case equation (1) has the form

$$\Delta\phi(x, y) = \frac{2\pi L}{\lambda} [n(x, y) - n_0], \tag{2}$$

where $L = z_2 - z_1$ is the depth of the transparent object being studied. The phase difference $\Delta\phi$ corresponds to a number of fringes k given by

$$k(x,y) = \frac{\Delta\phi}{2\pi} = \frac{L}{\lambda}[n(x,y) - n_0]. \tag{3}$$

If the fluid is a gas, the refractive index is a linear function of the gas density, expressed in the so-called Gladstone-Dale relation. The refractive index increment $[n(x,y) - n_0]$ in equation (3) then corresponds to a density increment $\Delta\rho$. If this density change is associated with a shock wave, it can be expressed as a function of the shock Mach number M_s with the help of the Rankine-Hugoniot equations [3]. Consequently one obtains

$$k = \frac{2({M_s}^2 - 1)}{(\gamma - 1){M_s}^2 + 2} \cdot \frac{K \cdot L \cdot \rho_0}{\lambda}, \tag{4}$$

where K is the fluid-specific Gladstone-Dale constant. In the case of weak shock waves ($M_s \approx 1$), the value for k according to equation (4) is small and the encountered variations of density are represented by less than one fringe (e.g., for $M_s = 1.01$, $L = 0.15\text{m}$, $K = 2.25 \times 10^{-4}\text{m}^3/\text{kg}$, $\gamma = 1.4$, $\rho_0 = 1.225\text{kg/m}^3$, and $\lambda = 694\text{nm}$ one gets $k = 0.994 \approx 1$). In principle it is possible to determine the value of these density changes by measuring the intensity variation across the fringe, but this result is rather inaccurate. The achievable resolution corresponds to one tenth of a fringe shift at best.

One possible way to overcome the described sensitivity limit of a regular holographic interferometer is to introduce multiple reference beams. The controlled manipulation of these reference beams during reconstruction of the recorded image allows one to determine phase differences with an accuracy of better than one hundredth of a fringe shift. The combination of this so-called heterodyne holographic interferometry with digital image processing is called digital phase-shift holographic interferometry. For most applications in flow visualization, a diffuse holographic interferogram is obtained, which allows one to observe the phenomenon from a range of viewing angles. This can be used to analyze - to some extent - the 3-D structure of a flow field, although in many cases the quantitative analysis of just one view suffices. The reconstructed image is digitally recorded and processed, which introduces a certain degree of automatization of the image evaluation.

2 Experimental

2.1 Generation of weak shock waves

Small explosive charges of silver azide (AgN_3) were used to generate weak shock waves. The charges (commercially available from Chyugoku-Kayaku Co. LTD) had masses between 0.5 mg and 10 mg. In a different test series the characteristics of the blast waves generated by these charges were determined [4]. The charges were ignited by the irradiation of a pulsed Nd:YAG laser (1064nm wavelength, 7ns nominal pulse duration, 25mJ nominal pulse energy). A preliminary

experiment had shown that the ignition threshold of these silver azide charges was below 100μJ with an ignition delay of less than 1μs [5].

Figure 1 is a schematic diagram of the weak shock generator. The AgN_3 charge was attached to an optical fiber (400μm core diameter) into which the Nd:YAG laser pulse was fed. The instant of firing of the laser, which corresponds with sufficient accuracy to the instant of ignition [5], was monitored by a photodiode. The Mach number of the generated shock waves was determined from a face-on overpressure measurement, conducted with a piezo-electric pressure transducer (Kistler 603B), which was mounted on a rigid plate facing the incoming shock wave. The pressure transducer and the charge were aligned on one axis with a distance of 236mm between them. A pulse generator provided a common trigger signal for both ignition and visualization. The synchronization between the arrival of the shock wave in the test section and the instant of visualization was achieved by two digital delay generators as seen in Fig. 1.

2.2 Digital phase-shift holographic interferometry

Figure 2 depicts schematically the optical arrangement used for the recording system. A double pulse ruby laser (λ = 694.3nm, nominal pulse energy 2J, nominal pulse duration 30ns) was used as light source. The system is essentially identical to a conventional holographic interferometer for diffuse illumination holograms. The light beam was split into object beam and reference beam by means of a beam splitter. The object beam was expanded by a concave lens before being scattered by the diffuser plate immediately in front of the test section. The reference beam was adjusted to have approximately the same optical path length as the object beam (accuracy: $\pm$10mm for a total path length of about 3.0m). It was finally expanded by means of a concave lens to completely fill the holographic recording plate.

The procedure of taking interferograms is the same as for conventional double pulse finite fringe interferograms [1]. The first holographic recording is taken before the shock waves are generated, i.e., at known reference conditions, while the second exposure is initiated with the phase object, i.e., the shock waves, present in the test section. Between exposures, one of the mirrors of the reference beam (see Fig. 2) is slightly tilted by an angle of about 0.05 degrees. In these tests, this tilting procedure was performed manually, which required a pulse separation of about one minute between exposures. By tilting the mirror, the holographic reference beam of the second exposure is different from the one of the first exposure, which is essential for the phase shift technique outlined above. The tilting of the mirror also produced a set of straight finite fringes, whose location in the reconstructed image was generally found to be behind the fringes generated by the phase object.

Figure 3 depicts schematically the optical arrangement used for the reconstruction system. The system corresponds essentially to a Michelson interferometer, where two reconstruction beams with small angular separation form a linear interference fringe pattern on the developed hologram plate. The angular

separation of the reconstruction beams is adjustable so that the generated linear fringe pattern can be set to coincide exactly with the previously recorded pattern of finite fringes on the hologram. The superposition of these two linear fringe systems produces a Moiré pattern except when the two fringe systems exactly overlap. The purpose of introducing this Moiré technique is to eliminate misalignment errors caused by the fact that recording and reconstruction setup are physically different. Furthermore, this alignment allows one to compensate for the chromatic errors that result from the wavelength difference between the recording and reconstruction lasers [6].

In order to introduce phase shifting, one plane mirror of the Michelson interferometer was mounted on a piezo-electrically movable transducer, which could be accurately displaced by known fractions of the laser wavelength. An objective lens with low F-number ($F = 1.4$) was chosen for the recording CCD camera and set close to the hologram so that the finite linear fringe pattern on the hologram was outside the image plane of the camera. As mentioned above, the finite fringe set does not appear in the same plane as the fringes associated with the phase object and can therefore be made to vanish from the image if the recording is performed with a low depth of field.

The camera output was digitized in real time by a frame grabber, an 8-bit A/D converter with programmable look-up table, and stored in a personal computer. Thus, during a video cycle, a digitized image was produced consisting of 640×480 (VGA) pixels, where every pixel was quantified in 8 bits, corresponding to 256 possible gray levels. This digitized image was then further processed according to image analysis and phase evaluation software.

In this study, four reconstructions of the hologram were carried out, each with a different phase shift introduced by the movable mirror (0°, 120°, 240°, and 360°). Thus each point of the image was recorded with four irradiance values (I_1, I_2, I_3, and I_4), corresponding to a phase of ϕ, $\phi + 120°$, $\phi + 240°$ and $\phi + 360°$, respectively. The unknown phase ϕ can be calculated from these irradiance values according to the Carré-formula [7]

$$\phi(x, y) = \arctan \frac{\sqrt{I_1 + I_2 - I_3 - I_4}\sqrt{3I_2 - 3I_3 - I_1 - I_4}}{I_2 + I_3 - I_1 - I_4}. \tag{5}$$

Theoretically, the images obtained at phase shifts of 0° and 360° should be identical so that $I_1 = I_4$, but usually small differences due to unwanted fluctuations exist, caused, e.g., by minute non-linearities in the mirror movement. The corresponding errors are compensated when the Carré-formula is used rather than the simpler expression for $I_1 = I_4$.

3 Results and Discussion

Figure 4 shows the measured pressure profile of the visualized shock wave together with a numerical prediction, indicated by the solid and the dotted line, respectively. A commercially available numerical code, AUTODYN 2-D, was used for the numerical calculation. As Fig. 4 shows, both results agree well except

that the numerically obtained overpressure exhibits more pronounced maximum and minimum values than the measured signal. This difference may be caused by the fact that the numerical scheme is an Euler code and that the modeling of the explosive may contain some uncertainties. According to Fig. 4, the peak face-on overpressure was 3.1kPa, from which one can determine the Mach number of the incident shock to $M_s = 1.007$ [3]. The incident wave is visualized approximately 15 mm before hitting the pressure transducer plate, i.e., at a distance of 221 mm from the charge. From other pressure measurements as well as from additional calculations and the results of a thorough characterization of these blast waves [4] it can be seen that the shock Mach number at the instant of visualization corresponds with sufficient accuracy to the value obtained from the overpressure measurement.

Figure 5(a) shows a sketch of the visualized shock waves as shown in Figs. 5(b) to 5(e). As outlined above, these four images represent four reconstructions of the same hologram. The differences of the intensity distribution are introduced by the described phase-shifting manipulation of the reference beams. In each image, the shock front is relatively easily recognized, but hardly any details can be discerned of the subsequent flow field. The density changes associated with these portions of the flow field are too small to be distinguishably resolved by a regular interferometer. According to the measured reflected overpressure of 3.1kPa, the normalized density change $\Delta\rho/\rho_0$ across the shock front is 0.00899 with $\rho_0 = 1.225\text{kg/m}^3$ at 15°C. The required density change for the generation of one interference fringe is $\Delta\rho/\rho_0 = 0.0084$, which follows from equation (3) together with the Gladstone-Dale relation for the same values of K, γ, and λ as used above and $L = 0.3\text{m}$. The shock front can therefore generate a visible interference effect, but other phenomena with weaker density changes remain almost invisible on each individual reconstructed image.

The combination of the four images (Figs. 5(b) to 5(e)), however, allows one to detect also phenomena with much smaller density variations than the shock front. Figure 6 presents the processed image that was obtained from Figs. 5(b) to 5(e) by applying equation (5) for each point of the images. This picture shows the phase map of the flow field, which can be 'unwrapped' in order to determine the density distribution in the test section. Figure 7 shows the result for the density distribution along the dotted line A-B in Fig. 6. The flow was assumed to be plane, which is sufficiently accurate. In this result, even the secondary shock wave generated by the explosion becomes clearly visible. The secondary shock is a feature that is characteristic of blast waves, but because of its usually diminutive amplitude it plays only a minor role in the analysis of blast wave flow fields. From the unwrapped phase map (Fig. 7) it can be seen that one of the disturbances associated with the secondary shock wave generates a density change of 0.0015kg/m^3. The shock Mach number that corresponds to this density change is $M_s \approx 1.0007$, which indicates that this disturbance is close to the acoustic limit. For comparison purposes the associated pressure change can be converted into sound intensity. The disturbance indicated in Fig. 7 generates a

pressure jump of about 135dB, which is almost equal to the noise generated by a rocket launch.

4 Conclusion

The present work has introduced digital phase shift holographic interferometry as a method suitable to measure minute density changes like those associated with very weak shock waves ($M_s \approx 1$). With the help of two reference beams and their controlled manipulation during the reconstruction of the image, the method-inherent sensitivity limit of a reference beam interferometer can be significantly lowered. The method was applied to visualize weak blast waves generated by milligram charges. Very weak density changes close to the acoustic limit could be resolved, which indicates the diagnostic potential of this technique for the investigation of compressible flows with small density changes.

References

1. Takayama K (1983) Application of holographic interferometry to shock wave research. In: Proc. SPIE **398**:174–180
2. Merzkirch W (1974) Flow visualization. Academic, Orlando
3. Liepmann W, Roshko A (1956) Elements of Gasdynamics. John Wiley, London
4. Ohashi K, Kleine H, Takayama K (2001) *Characteristics of blast waves generated by milligram charges*, these proceedings
5. Mizukaki T (2001) *Quantitative visualization of shock waves.* Doctoral thesis, Tohoku University, Sendai (in Japanese)
6. Breuckmann B and Thieme W (1985) *Computer-aided analysis of holographic interferograms using the phase shift method*, Applied Optics **24**:824-831
7. Robinson D, Reid G (eds.) (1993) Interferogram analysis. Institute of Physics Publishing, Philadelphia

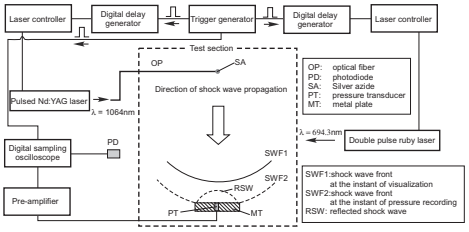

Fig. 1. Schematic diagram of weak shock wave generator

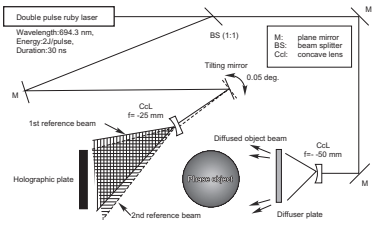

Fig. 2. Schematic diagram of the recording system of digital phase shift interferometry

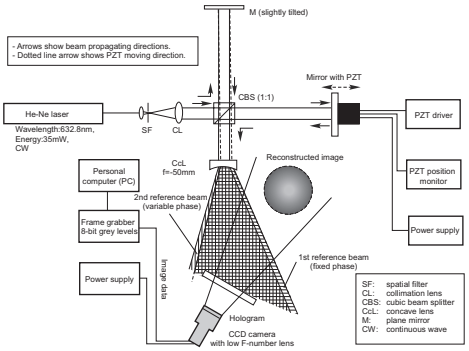

Fig. 3. Schematic diagram of the reconstruction setup

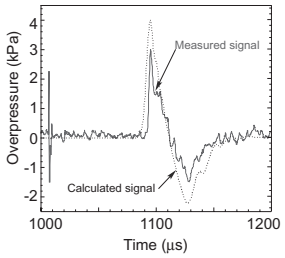

Fig. 4. Measured and calculated overpressure profiles

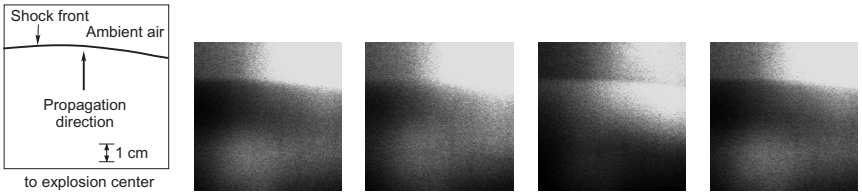

(a) Sketch of flow field (b) I_1 (c) I_2 (d) I_3 (e) I_4

Fig. 5. Reconstructed images with phase shifts $\Delta\phi = 0°$ (b), $\Delta\phi = 120°$ (c), $\Delta\phi = 240°$ (d), $\Delta\phi = 360°$ (e)

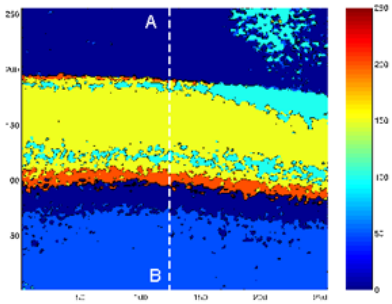

Fig. 6. Processed phase map

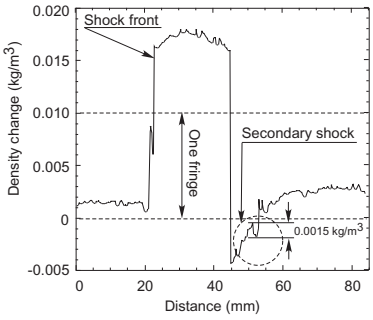

Fig. 7. Density distribution obtained from phase map